Electrochemical Properties of 1,3-Dimethylimidazolium Dicyanamide, Bis(trifluoromethanesulfonyl)imide and Dimethylphosphate Ionic Liquids

Yong Zheng[1,], Yongjun Zheng[1], Qian Wang[2], Huichao Lv[1], Zhen Wang[1]*

[1] College of Chemical and Environmental Engineering, Anyang Institute of Technology, Anyang 455000, P. R. China
[2] State Key Laboratory of Multiphase Complex Systems, Institute of Process Engineering, Chinese Academy of Sciences, Beijing 100190, P. R. China
[*]E-mail: yzheng83@126.com

1,3-dimethylimidazolium-based ionic liquids show promise as electrolytes because of their special cation structure. However, their electrochemical properties remain less understood. Thus, 1,3-dimethylimidazolium dicyanamide, bis(trifluoromethanesulfonyl)imide and dimethylphosphate were chosen as representative 1,3-dimethylimidazolium-based ionic liquids in this work. The electrical conductivity and molar conductivity of these ionic liquids were measured and calculated from 303.15 to 353.15 K, which were well fitted with empirical equations. Meanwhile, the corresponding electrochemical window and differential capacitance were also obtained by cyclic voltammetry and impedance measurements, respectively. On the basis of experimental data and theoretical calculations, the relationships between the electrochemical properties and molecular structures of the ionic liquids were assessed in detail. These ionic liquids have higher electrical conductivity and wider electrochemical windows than many other 1-alkyl-3-methylimidaozlium-based ionic liquids with the same anions. These phenomena are probably ascribed to the higher structural symmetry, stronger cation–anion interaction and smaller size of the 1,3-dimethylimidazolium cation. Moreover, 1,3-dimethylimidazolium dicyanamide has a higher dissociation of ions, while 1,3-dimethylimidazolium bis(trifluoromethanesulfonyl)imide and dimethylphosphate have a lower ionic dissociation. 1,3-dimethylimidazolium cations are prone to be adsorbed onto the Pt plate electrodes when the cation–anion interaction is lower. It is hoped that the present work will provide important electrochemical research results for the future application of these ionic liquids.

1. INTRODUCTION

Ionic liquids (ILs) are regarded as novel low-temperature molten salts, which usually consist of organic cations and monovalent anions. Owing to their excellent physicochemical properties, ILs have already been employed as green electrolytes, solvents, catalysts and absorbents in a variety of scientific fields [1-3].

1-alkyl-3-methylimidaozlium-based molten salts are one of the most popular and reported classes of ILs. The widespread usage of these ILs is mainly due to their relatively lower melting points, broader electrochemical window, higher electrical conductivity and superior chemical stability [4]. Until now, the most studied *N*-alkyl chains of 1-alkyl-3-methylimidaozlium-based ILs include ethyl, butyl and hexyl groups [5-12]. Remarkable research progress has been achieved in the electrochemistry of these ILs over the past two decades. For example, 1-ethyl-3-methylimidazolium dicyanamide and 1-butyl-3-methylimidazolium dibutylphosphate have been applied in the low-temperature electrodeposition of nickel, zinc, copper and tin [7-9]. 1-Ethyl-3-methylimidazolium and 1-butyl-3-methylimidazolium bis(trifluoromethanesulfonyl)imide can be used in electroanalytical chemistry, electrochemical preparation and supercapacitors [10-12].

Our previous work and literature survey both reveal that decreasing the *N*-alkyl chain length could improve the electrical conductivity and chemical stability of 1-alkyl-3-methylimidaozlium-based ILs [13,14]. It should be pointed out that the shortest alkyl chain for these ILs is the methyl group, where the cation is well known as 1,3-dimethylimidazolium. Therefore, the special molecular structure of the cation makes 1,3-dimethylimidazolium-based ILs attractive as promising electrolytes in electrochemistry. However, only a few 1,3-dimethylimidazolium-based ILs have been prepared and reported in the literature [15-17]. The electrochemical properties of 1,3-dimethylimidazolium-based ILs remain understood. Meanwhile, the investigations on the corresponding relationship between their electrochemical features and molecular structure are also limited. To promote relevant research and application, more efforts are required to invest in the electrochemical exploration of 1,3-dimethylimidazolium-based ILs.

Inspired by the above research background, we aim to conduct further systematic studies on the typical electrochemical properties and molecular structure of 1,3-dimethylimidazolium-based ILs by experimental measurements and theoretical calculation methods. Accordingly, three representative 1,3-dimethylimidazolium-based ILs with different anions, including 1,3-dimethylimidazolium dicyanamide ([Mmim][N(CN)$_2$]), 1,3-dimethylimidazolium bis(trifluoromethanesulfonyl)imide ([Mmim][NTf$_2$]) and 1,3-dimethylimidazolium dimethylphosphate ([Mmim][DMP]), were studied in this work. The electrical conductivity and molar conductivity of these ILs were measured and calculated from 303.15 to 353.15 K at 101.3 kPa, which were fitted by empirical equations. Meanwhile, the corresponding electrochemical window and differential capacitance of ILs at the Pt electrode were also investigated. Theoretical calculations were also performed by the Gaussian 09W program to obtain deeper insight into the structure of the ILs. On the basis of experimental data and theoretical calculations, the relationships between these electrochemical properties and molecular structures were analysed and discussed in detail.

2. EXPERIMENTAL PROCEDURE

2.1 Chemicals

[Mmim][NTf$_2$], [Mmim][DMP], 1,3-dimethylimidazolium chloride ([Mmim]Cl), and 1-butyl-3-methylimidazolium bis(trifluoromethanesulfonyl)imide ([Bmim][NTf$_2$]) were purchased from the Shanghai Macklin Biochemical Co., Ltd. Sodium dicyanamide, acetone, dichloromethane, acetonitrile, sulfuric acid, hydrochloric acid and silver nitrate were provided by the Sinopharm Chemical Reagent Co., Ltd. [Mmim][N(CN)$_2$] was synthesized according to our previous work [13]. [Mmim][NTf$_2$], [Mmim][DMP] and [Bmim][NTf$_2$] were purified by recrystallization and vacuum drying before use.

2.2 Characterization of ILs

The characterization of [Mmim][NTf$_2$], [Mmim][DMP] and [Mmim][N(CN)$_2$] was performed through NMR spectrometry (av-400 MHz, Bruker), infrared spectrometry (Nicolet iS10, Thermo), elemental analysis (Vario El cube, Elementar) and Karl Fisher titration (751 GPD Titrino, Metrohm). The structure and chemical composition of the ILs were confirmed by these measurements. The mass fraction purity of the ILs was higher than 0.995, and the water content was below 50 mg/kg.

2.3 Electrochemical measurements

All electrochemical measurements were conducted in an argon-filled glove box (LABstar, Mbraun), where the mass contents of water and oxygen were both below 1 mg/kg. The atmospheric pressure was controlled at 101.3 kPa by a programmable logic controller in the glove box, and the experimental temperature was regulated by a thermostat (HRC 2 control, IKA) with a stability of ±0.05 K. The electrical conductivity of ILs was measured from 303.15 to 353.15 K by a conductivity meter (FE38, Mettler Toledo), which was equipped with a conductivity sensor (InLab710, Mettler Toledo). Controlled by an electrochemical workstation (CHI660E, Chenhua), a three-electrode cell was applied in the cyclic voltammetry and differential capacitance experiments. The corresponding experimental temperature was 303.15 K, which was controlled by the thermostat. Pt plate electrodes (Pt255, Ida) were used as working and counter electrodes. A nonaqueous Ag$^+$/Ag electrode (R0201, Ida) containing a 0.01 mol/kg solution of silver nitrate in [Bmim][NTf$_2$]/acetonitrile was prepared as the reference electrode. Before use, Pt plate electrodes were polished with alumina powder, treated with a dilute sulfuric acid/hydrochloric acid mixture, cleaned with ethanol, and dried under vacuum.

2.4 Density and viscosity measurements

The density of ILs was measured by a vibrating tube density meter (DMA 5000 M, Anton Paar) from 303.15 to 353.15 K at 101.3 kPa. The temperature precision and repeatability of density were ±0.01 K and 0.000001 g, respectively. The viscosity measurement was conducted by an automated viscometer (Lovis 2000 ME, Anton Paar) at 101.3 kPa, and the temperature precision and accuracy of

viscosity were ±0.01 K and 0.5%, respectively. These measurements were conducted in a glove box, and the atmospheric pressure was regulated by a programmable logic controller. The mass measurement was conducted by a microbalance with 0.000001 g accuracy (XP6, Mettler Toledo).

2.5 Theoretical calculation

Theoretical calculations for [Mmim][N(CN)$_2$], [Mmim][NTf$_2$] and [Mmim][DMP] ILs were performed with the Gaussian 09W program, which was based on the well-known density functional theory (DFT). Becke−three−parameter−Lee−Yang−Parr (B3LYP) with a 6-311++G(d,p) basis set was applied in the optimization of ILs [18]. Each structure of ion pairs was optimized and obtained with the minimum energy by frequency calculation. The counterpoise method was used to estimate the basis set superposition errors (BSSE) for the interaction energy. The final geometries of ion pairs were confirmed by vibrational analysis to ensure that no imaginary frequency existed in the calculation [19].

3. RESULTS AND DISCUSSION

3.1 Electrical conductivity

The experimental electrical conductivity of the ILs and the temperature dependency of these data are shown in Figure 1. All values of electrical conductivity κ range from 3.47 to 104.01 mS/cm, which are well fitted by the well-known Vogel–Fulcher–Tammann (VFT) equation at different temperatures T. In Equation 1, κ_0, B and T_0 are VFT empirical parameters [20,21]. The fitted values of these parameters and corresponding standard deviations are presented in Table 1.

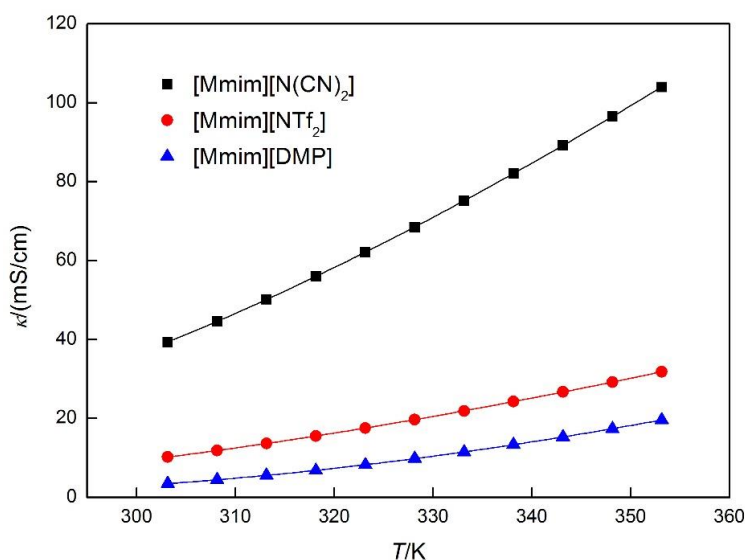$$\kappa = \kappa_0 \exp(\frac{B}{T_0 - T}) \qquad\qquad (1)$$

Figure 1. Electrical conductivity κ of 1,3-dimethylimidazolium-based ILs measured at different temperatures T. The solid curves are correlated with Equation 1.

Table 1. Fitted parameters κ_0, B, T_0 and corresponding standard deviation σ for the experimental electrical conductivity of ILs based on Equation 1.

IL	κ_0/(mS/cm)	B/K	T_0/K	σ
[Mmim][N(CN)$_2$]	1951.1	588.6	152.4	0.0321
[Mmim][NTf$_2$]	687.64	569.2	167.9	0.0192
[Mmim][DMP]	615.01	515.8	203.5	0.0119

As Figure 1 illustrates, the electrical conductivity of the ILs increases rapidly with increasing temperature. A similar temperature dependency of electrical conductivity can also be observed for many other common ILs. This reflects that the transfer of ionic charge is significantly enhanced under such conditions. This phenomenon is mainly attributed to the weaker electrostatic force, lower viscosity and stronger thermal motion of ions at higher temperatures [22].

It is interesting to note that these ILs are more electrically conductive than many other 1-alkyl-3-methylimidaozlium-based ILs when they contain the same anions at the same temperature. For example, the electrical conductivity of [Mmim][N(CN)$_2$] is 39.34 mS/cm at 303.15 K, while the experimental values of 1-ethyl-3-methylimidaozlium dicyanamide ([Emim][N(CN)$_2$]) and 1-butyl-3-methylimidaozlium dicyanamide ([Bmim][N(CN)$_2$]) are 32.23 and 13.90 mS/cm at the same temperature, respectively [23,24]. This confirms that a decrease in the *N*-alkyl chain length could improve the ionic conductivity of ILs, which is consistent with our previous work [13].

Theoretical calculations were performed to investigate the relationship between the molecular structure and electrochemical properties of the ILs. As Figure 2 and Table 2 show, the 1,3-dimethylimidazolium cation has higher structural symmetry and smaller size than many other 1-alkyl-3-methylimidaozlium cations [18,19]. It can be inferred that the special structural features of 1,3-dimethylimidazolium promote charge transfer and ion mobility in ILs.
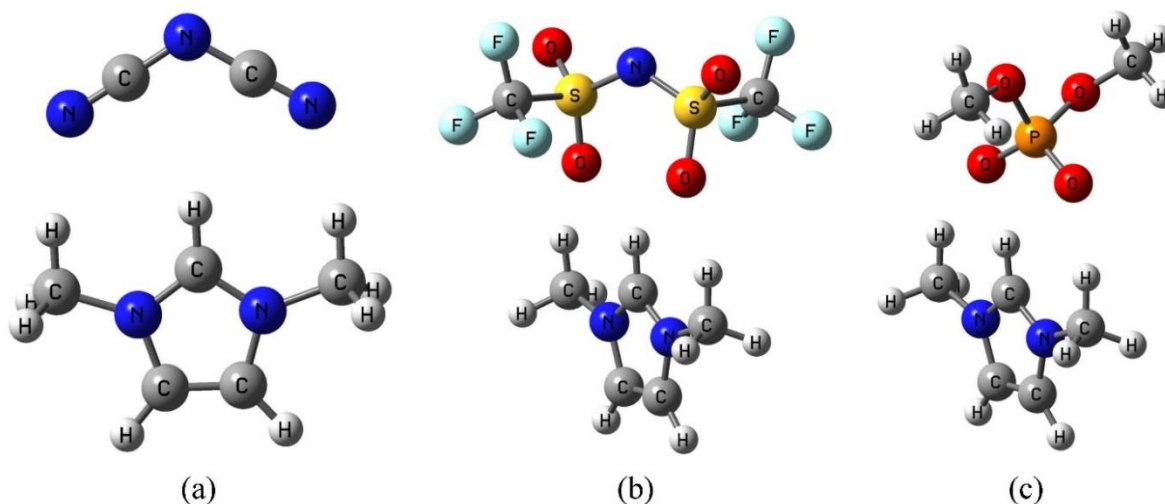

Figure 2. The optimized structure of ion pairs for 1,3-dimethylimidazolium-based ILs obtained by theoretical calculation. (a) [Mmim][N(CN)$_2$]; (b) [Mmim][NTf$_2$]; (c) [Mmim][DMP].

Table 2. Structural parameters of ion pairs for 1,3-dimethylimidazolium-based ILs obtained by theoretical calculation.

IL[a]	$R^{b}/(10^{-10}$ m)	$V^{c}/(10^{-28}$ m^3)	$\Delta E^{d}/$(kJ/mol)
[Mmim][N(CN)$_2$]	2.87	2.19	329.91
[Mmim][NTf$_2$]	3.55	3.75	331.62
[Mmim][DMP]	3.19	2.82	404.07

[a]average radius of 1,3-dimethylimidazolium cation = 3.30×10^{-10} m; [b]average radius of anion; [c]average volume of ion pair; [d]cation–anion interaction energy

The type of anion also has a significant effect on the ionic conductivity of 1,3-dimethylimidazolium-based ILs. As Figure 1 shows, the electrical conductivity of the ILs at the same temperature follows the order [Mmim][N(CN)$_2$] > [Mmim][NTf$_2$] > [Mmim][DMP]. In contrast, the interaction energy and viscosity of the ILs change in an opposite trend, [Mmim][N(CN)$_2$] < [Mmim][NTf$_2$] < [Mmim][DMP], according to Table 2 and experimental measurements. For instance, the viscosities of [Mmim][N(CN)$_2$], [Mmim][NTf$_2$] and [Mmim][DMP] at 303.15 K are 11.98, 30.80 and 195.44 mPa·s, respectively. This reveals that a weaker interaction among ions and a lower viscosity of ILs could increase the electrical conductivity. Obviously, the electrical conductivity of [Mmim][N(CN)$_2$] is higher than that of [Mmim][NTf$_2$] and [Mmim][DMP] under the same conditions.

Table 3. Density ρ of 1,3-dimethylimidazolium-based ILs measured at temperature T = (303.15 to 353.15) K and 101.3 kPa.

	$\rho/$(g/cm^3)		
T/K	[Mmim][N(CN)$_2$]	[Mmim][NTf$_2$]	[Mmim][DMP]
303.15	1.131986	1.563584	1.251504
308.15	1.128528	1.558394	1.248049
313.15	1.125091	1.553230	1.244601
318.15	1.121675	1.548089	1.241174
323.15	1.118279	1.542969	1.237767
328.15	1.114901	1.537871	1.234376
333.15	1.111542	1.532798	1.231007
338.15	1.108200	1.527746	1.227640
343.15	1.104877	1.522710	1.224295
348.15	1.101568	1.517694	1.220958
353.15	1.098272	1.512697	1.217636

Molar conductivity was calculated to evaluate the efficiency of 1,3-dimethylimidazolium-based ILs in conducting electricity. The values of molar conductivity Λ were obtained by Equation 2, in

which M and ρ stand for the molar weight and density of the ILs, respectively [25]. Table 3 lists the density of 1,3-dimethylimidazolium-based ILs measured at different temperatures.

$$\Lambda = \frac{\kappa M}{\rho} \qquad (2)$$

Figure 3 illustrates the molar conductivity of the ILs calculated by Equation 2 and the temperature dependency of these data. All experimental data fit well with the VFT equation. As expressed by Equation 3, Λ_0, B and T_0 are empirical VFT parameters [26,27]. The fitted values of these parameters and corresponding standard deviations are presented in Table 4.

$$\Lambda = \Lambda_0 \exp(\frac{B}{T_0 - T}) \qquad (3)$$

As Figure 3 shows, the molar conductivity of the ILs increases in the range of 0.62 and 12.56 S·cm^2/mol when temperature rises from 303.15 to 353.15 K. This trend is the same as that of electrical conductivity, which results from the increase in ionic conductivity and IL molar volume. This reflects that the ability of ions to conduct electricity per unit molar concentration of ILs is enhanced at higher temperatures.
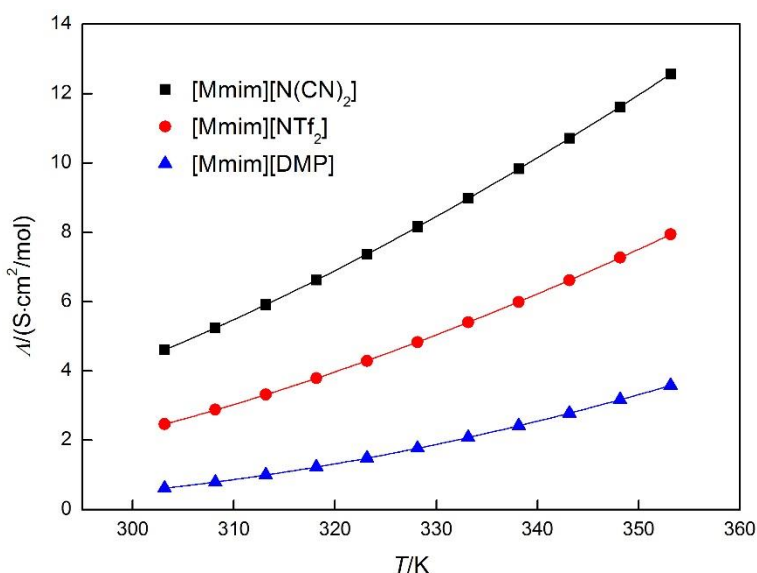

Figure 3. Molar conductivity Λ of 1,3-dimethylimidazolium-based ILs obtained at different temperatures T. The solid curves are correlated with Equation 3.

Table 4. Fitted parameters Λ_0, B, T_0 and corresponding standard deviation σ for the experimental molar conductivity of ILs based on Equation 3.

IL	Λ_0/(S·cm^2/mol)	B/K	T_0/K	σ
[Mmim][N(CN)$_2$]	278.2	633.1	148.8	0.0026
[Mmim][NTf$_2$]	199.6	605.7	165.3	0.0060
[Mmim][DMP]	130.8	549.4	200.5	0.0027

Compared with electrical conductivity, the molar conductivity of 1,3-dimethylimidazolium-based ILs also follows the order [Mmim][N(CN)$_2$] > [Mmim][NTf$_2$] > [Mmim][DMP] under the same experimental conditions. It should be noted that the differences among the molar conductivities of these ILs are smaller than those among the electrical conductivities. This phenomenon mainly results from the various molar volumes, densities and molecular weights of ILs. For example, the molar volumes of [Mmim][N(CN)$_2$], [Mmim][NTf$_2$] and [Mmim][DMP] at 303.15 K are 117.14, 241.29 and 177.53 cm^3/mol, respectively. As Table 2 shows, the order of molar volume is the same as that of the ion pairs' average volume, which confirms the theoretical calculation results.

3.2 Cyclic voltammetry

Cyclic voltammetry measurements were conducted to further explore the electrochemical properties of the 1,3-dimethylimidazolium-based ILs. Figure 4 demonstrates the cyclic voltammograms recorded in these ILs. It is apparent that all voltammograms display a couple of classic oxidation and reduction peaks. The oxidation peaks at positive potentials are ascribed to the oxidation process of IL anions, while the reduction peaks at negative potentials result from the electrochemical reduction of 1,3-dimethylimidazolium cations.
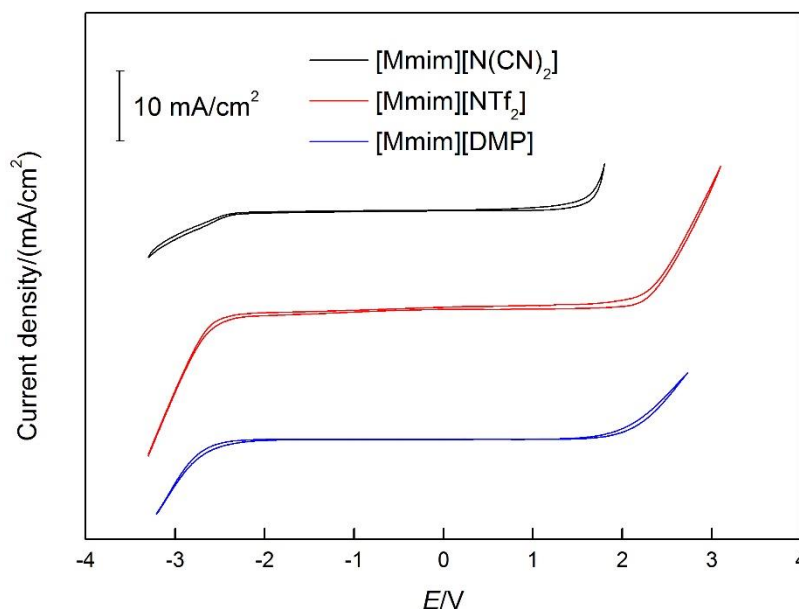

Figure 4. Cyclic voltammograms obtained at the Pt plate electrode in 1,3-dimethylimidazolium-based ILs at 303.15 K and 101.3 kPa with a potential scan rate of 50 mV/s.

The electrochemical windows of these ILs are generally higher than 4 V, which are also wider than those of many other 1-alkyl-3-methylimidazolium-based ILs containing the same anions [7,28-30]. For example, the electrochemical window of [Mmim][NTf$_2$] reaches approximately 5 V, while that of [Bmim][NTf$_2$] is approximately 4 V [30]. This confirms the fact that 1,3-dimethylimidazolium-based

ILs have higher electrochemical stability, which may probably result from the relatively strong cation–anion interaction and stable cation. Based on the above experimental results and theoretical calculations, it can be concluded that the higher structural symmetry, shorter *N*-alkyl chain and smaller volume of the 1,3-dimethylimidazolium cation enhance the binding force and electrochemical stability of ILs.

As Figure 4 shows, the reduction potentials of these ILs are all approximately −2.5 V and close to each other. This indicates that the 1,3-dimethylimidazolium cations of these ILs lead to approximately equal reduction potentials. On the other hand, the oxidation potentials of these ILs are quite different and follow the order [Mmim][NTf$_2$] > [Mmim][DMP] > [Mmim][N(CN)$_2$], implying that the electrochemical stability of the [NTf$_2$]$^-$ anion is higher than that of [DMP]$^-$ and [N(CN)$_2$]$^-$ anions. In view of the relationship between the molecular structure and physicochemical properties, it is proper to state that the presence of a fully fluorinated anion [NTf$_2$]$^-$ improves the electrochemical stability of ILs [31]. In addition, the stronger cation–anion interaction and relatively saturated molecular structure of the [DMP]$^-$ anion could probably lead to higher electrochemical stability of [Mmim][DMP] than that of [Mmim][N(CN)$_2$].

3.3 Differential capacitance

An electrical double layer is widespread at the electrode–IL interface, and is closely related to the molecular size, absorption behaviour and electrostatic force of ions. Differential capacitance is important to the understanding of IL electrochemical properties and the corresponding electrical double layer [1,32]. Thus, impedance measurements were conducted within electrochemical windows according to the results of cyclic voltammograms in this work. The experimental potential was scanned from the cathodic to anodic potential limit at the same temperature, and the corresponding experimental frequency ranged from 1 to 5×10^4 Hz. On the basis of impedance data, the differential capacitance (C_d) of 1,3-dimethylimidazolium-based ILs was obtained according to Equation 4, in which *f* and *Z″* represent the experimental frequency and imaginary part of impedance, respectively [33-35].

$$C_d = -\frac{1}{2\pi f Z''} \qquad (4)$$

The capacitance–potential curves recorded in 1,3-dimethylimidazolium-based ILs are shown in Figure 5. Obviously, the curve obtained in [Mmim][N(CN)$_2$] exhibits a bell shape, as reported for pure electrolytes. This reveals that [Mmim][N(CN)$_2$] has a higher dissociation of ions with a lattice saturation degree $\gamma > 1/3$ [36]. According to our previous research and experience, the ionic dissociation of 1-alkyl-3-methylimidaozlium dicyanamide is higher than that of other common ILs containing the same cations. Therefore, dicyanamide-based ILs have much higher electrical conductivity. Meanwhile, the capacitance–potential curves obtained in [Mmim][NTf$_2$] and [Mmim][DMP] are camel-shaped with $\gamma < 1/3$, indicating the presence of lower ionic dissociation [37]. This confirms the fact that [Mmim][NTf$_2$] and [Mmim][DMP] have lower electrical conductivity and higher cation–anion interaction energy, as described above.

As Figure 5 shows, these 1,3-dimethylimidazolium-based ILs have relatively smaller differences in differential capacitance at negative potentials, which is probably attributed to the same cation of ILs. In contrast, the capacitance data of these ILs are quite different from each other at positive potentials, which may result from the various chemical compositions and structures of $[N(CN)_2]^-$, $[NTf_2]^-$ and $[DMP]^-$ anions. According to Table 2, the average radius of anions changes in the order $[N(CN)_2]^- < [DMP]^- < [NTf_2]^-$. It can be concluded that the difference in these anions' structure and size could lead to different structures of electrical double layers on the Pt electrode surface.
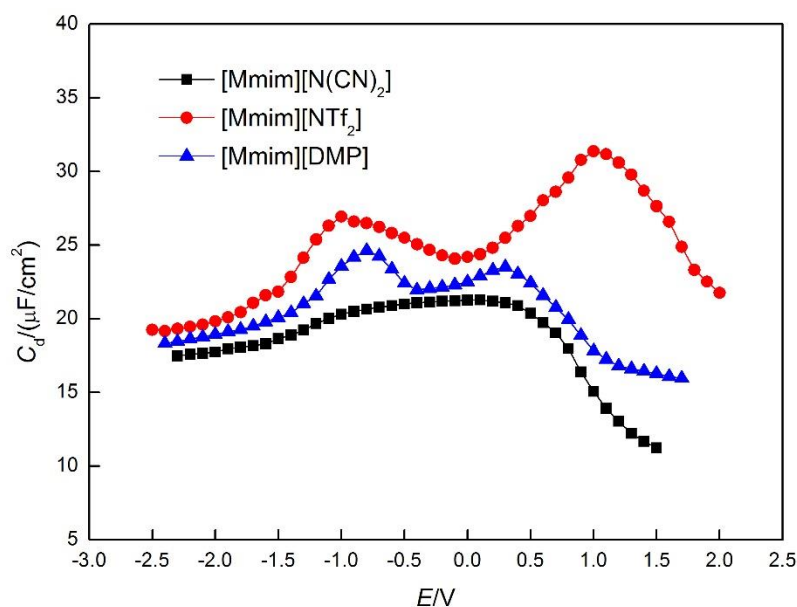

Figure 5. Capacitance-potential curves obtained at the Pt plate electrode in 1,3-dimethylimidazolium-based ILs at 303.15 K and 101.3 kPa.

Figure 5 also shows that these ILs have different potentials of zero charge (PZC) [38]. The PZC of $[Mmim][N(CN)_2]$ is obtained from the maximum capacitance (bell shape), while the PZC values of $[Mmim][NTf_2]$ and $[Mmim][DMP]$ are determined at the minimum between the two maxima of capacitance (camel shape) [35,39]. The PZC values of the ILs follow the order $[Mmim][N(CN)_2]$ (0.1 V) > $[Mmim][NTf_2]$ (−0.1 V) > $[Mmim][DMP]$ (−0.4 V). This indicates that the $[Mmim]^+$ cation of these ILs is prone to be adsorbed onto the Pt plate electrode when the cation–anion interaction is lower. Accordingly, no excess charge on the electrode interface is obtained at a higher potential for $[Mmim][N(CN)_2]$. When the experimental potential is far from PZC, IL ions are not sufficient to compensate for the excess surface charge on the electrode. Under this condition, the differential capacitance of ILs decreases as a function of potential. The camel shape of the capacitance curves also indicates the specific adsorption of anions in $[Mmim][NTf_2]$ and $[Mmim][DMP]$ at positive potentials [32].

4. CONCLUSIONS

In this work, a systematic study was carried out on the typical electrochemical properties of three 1,3-dimethylimidazolium-based ILs. The values of electrical conductivity and molar conductivity are well fitted with the classic VFT equation, which follows the order [Mmim][N(CN)$_2$] > [Mmim][NTf$_2$] > [Mmim][DMP]. These ILs have higher electrical conductivity and electrochemical windows than many other 1-alkyl-3-methylimidaozlium-based ILs when they contain the same anions. Based on experimental results and theoretical calculations, these phenomena are probably ascribed to the higher structural symmetry, stronger cation–anion interaction and smaller size of the 1,3-dimethylimidazolium cation. The presence of fully fluorinated anion [NTf$_2$]$^-$ could improve the electrochemical stability of ILs. In addition, the differential capacitance data reflect that [Mmim][N(CN)$_2$] has a higher dissociation of ions with $\gamma > 1/3$, while [Mmim][NTf$_2$] and [Mmim][DMP] have a lower ionic dissociation with $\gamma > 1/3$. The PZC values of the ILs follow the order [Mmim][N(CN)$_2$] > [Mmim][NTf$_2$] > [Mmim][DMP], implying that the [Mmim]$^+$ cation is prone to be adsorbed onto the Pt plate electrode when the cation–anion interaction is lower. It is hoped that the present work will provide important electrochemical research results for the future application of 1,3-dimethylimidazolium-based ILs.

References

1. M. V. Fedorov and A. A. Kornyshev, *Chem. Rev.*, 114 (2014) 2978
2. C. Dai, J. Zhang, C. Huang and Z. Lei, *Chem. Rev.*, 117 (2017) 6929
3. S. Zeng, X. Zhang, L. Bai, X. Zhang, H. Wang, J. Wang, D. Bao, M. Li, X. Liu and S. Zhang, *Chem. Rev.*, 117 (2017) 9625
4. H. L. Ngo, K. LeCompte, L. Hargens and A. B. McEwen, *Thermochim. Acta*, 357-358 (2000) 97
5. J. K. Singh, R. K. Sharma, P. Ghosh, A. Kumar and M. L. Khan, *Front. Chem.*, 6 (2018) 548
6. A. L. Sanati and F. Faridbod, *Int. J. Electrochem. Sci.*, 12 (2017) 7997
7. M. J. Deng, P. Y. Chen, T. I. Leong, I. W. Sun, J. K. Chang and W. T. Tsai, *Electrochem. Commun.*, 10 (2008) 213
8. Y. Zheng, X. Zhou, Y. Luo and P. Yu, *RSC Adv.*, 10 (2020) 16576
9. M. Xu, D. G. Ivey, W. Qu and Z. Xie, *J. Power Sources*, 274 (2015) 1249
10. G. Murali Krishna, A. S. Suneesh, K. A. Venkatesan and M. P. Antony, *J. Electroanal. Chem.*, 776 (2016) 120
11. Shalu, V. K. Singh and R. K. Singh, *J. Mater. Chem. C*, 3 (2015) 7305
12. L. Dagousset, G. Pognon, G. T. M. Nguyen, F. Vidal, S. Jus and P. H. Aubert, *J. Power Sources*, 359 (2017) 242
13. Y. Zheng, Y. Zheng, Q. Wang and Z. Wang, *J. Chem. Eng. Data*, 66 (2021) 480
14. O. Nordness and J. F. Brennecke, *Chem. Rev.*, 120 (2020) 12873
15. S. Bahrani, S. Raeissi and M. Sarshar, *Biores. Technol.*, 185 (2015) 411

16. W. Xiao, Q. Chen, Y. Wu, T. Wu and L. Dai, *Carbohydr. Polym.*, 83 (2011) 233
17. J. D. Holbrey, W. M. Reichert and R. D. Rogers, *Dalton Trans.*, 15 (2004) 2267
18. D. K. Singh, B. Rathke, J. Kiefer and A. Materny, *J. Phys. Chem. A*, 120 (2016) 6274
19. M. R. Housaindokht, H. E. Hosseini, M. S. S. Googheri, H. Monhemi, R. I. Najafabadi, N. Ashraf and M. Gholizadeh, *J. Mol. Liq.*, 177 (2013) 94
20. L. F. Zubeir, M. A. A. Rocha, N. Vergadou, W. M. A. Weggemans, L. D. Peristeras, P. S. Schulz, I. G. Economou and M. C. Kroon, *Phys. Chem. Chem. Phys.*, 18 (2016) 23121
21. Y. Zheng, K. Dong, Q. Wang, J. Zhang and X. Lu, *J. Chem. Eng. Data*, 58 (2013) 32
22. L. Xu, X. Cui, Y. Zhang, T. Feng, R. Lin, X. Li and H. Jie, *Electrochim. Acta*, 174 (2015) 900
23. P. D. A. Bastos, F. S. Oliveira, L. P. N. Rebelo, A. B. Pereiro and I. M. Marrucho, *Fluid Phase Equilib.*, 389 (2015) 48
24. N. Zec, M. Bešter-Rogač, G. Marolt, M. Vraneš and S. Gadžurić, *J. Chem. Thermodyn.*, 101 (2016) 293
25. D. Rauber, F. Philippi, J. Zapp, G. Kickelbick, H. Natter and R. Hempelmann, *RSC Adv.*, 8 (2018) 41639
26. Q. S. Liu, M. Yang, P. P. Li, S. S. Sun, U. Welz-Biermann, Z. C. Tan and Q. G. Zhang, *J. Chem. Eng. Data*, 56 (2011) 4094
27. M. S. Miran, H. Kinoshita, T. Yasuda, M. A. B. H. Susan and M. Watanabe, *Phys. Chem. Chem. Phys.*, 14 (2012) 5178
28. R. Costa, C. M. Pereira and F. Silva, *Phys. Chem. Chem. Phys.*, 12 (2010) 11125
29. F. T. Chen, B. Wang and H. Z. Ma, *J. Hazard. Mater.*, 165 (2009) 1253
30. R. Michez, J. V. Steen, T. Doneux, M. Luhmer and C. Buess-Herman, *Electrochim. Acta*, 270 (2018) 434
31. F. Endres and S. Z. E. Abedin, *Phys. Chem. Chem. Phys.*, 8 (2006) 2101
32. V. Lockett, M. Horne, R. Sedev, T. Rodopoulos and J. Ralston, *Phys. Chem. Chem. Phys.*, 12 (2010) 12499
33. Y. Su, J. Yan, M. Li, M. Zhang and B. Mao, *J. Phys. Chem. C*, 117 (2013) 205
34. Y. Zheng, Y. Zheng, C. Peng, Z. Zhao and D. Tian, *Int. J. Electrochem. Sci.*, 11 (2016) 9585
35. Q. Zhang, Y. Han, Y. Wang, S. Ye and T. Yan, *Electrochem. Commun.*, 38 (2014) 44
36. Y. Z. Su, Y. C. Fu, Y. M. Wei, J. W. Yan and B. W. Mao, *ChemPhysChem*, 11 (2010) 2764
37. A. A. Kornyshev, N. B. Luque and W. Schmickler, *J. Solid State Electrochem.*, 18 (2014) 1345
38. Q. Dou, L. Liu, B. Yang, J. Lang and X. Yan, *Nat. Commun.*, 8 (2017) 2188
39. E. Paek, A. J. Pak and G. S. Hwang, *J. Electrochem. Soc.*, 160 (2013) A1